



## PREFABRICATED SFRC JACKETS FOR SEISMIC RETROFIT OF NON-DUCTILE REINFORCED CONCRETE COLUMNS

Alper ILKI<sup>1</sup> Esen YILMAZ<sup>2</sup> Cem DEMIR<sup>3</sup> Nahit KUMBASAR<sup>4</sup>

### SUMMARY

In this study an experimental work was carried out on the inelastic behavior of non-ductile column confining zones and retrofitting of these zones with prefabricated steel fiber reinforced concrete (SFRC) panels. Six specimens were constructed with low strength concrete ( $f'_c=9.22$  MPa) and inadequate transverse reinforcement. Both longitudinal and transverse reinforcement were plain bars. These specimens were tested under the combined effect of constant axial load and reversed cyclic lateral loads. Three of these specimens had continuous longitudinal reinforcement while the other three had inadequate lap splices. Two specimens from each group were retrofitted with prefabricated SFRC panels of altering thicknesses. It was observed that both reference specimens, which were not retrofitted, presented premature loss of performance either due to buckling of longitudinal reinforcement or loss of bond, while retrofitted ones exhibited a superior performance. The improvement was in terms of ductility, strength, and failure mode.

### INTRODUCTION

In recent years, seismic design provisions were revised considering performance based design in order to ensure a satisfactory performance for the newly designed reinforced concrete structures. However, there are many existing structures designed and constructed according to older codes and older methodologies for some of which only vertical loads were considered during design. Thus these structures do not comply with the lateral strength and ductility requirements of the recent seismic codes. In the last 30 years several destructive earthquakes (for example, 1978 Miyagiken-oki, 1985 Mexico, 1989 Loma Prieta, 1994 Northridge, 1995 Kobe, 1999 Adapazari) hit populated areas, leaving behind enormous life and/or financial losses. Just in the year 2003, 32819 earthquake deaths worldwide have been confirmed by the United Nations Office for Coordination of Humanitarian Affairs, USGS [1].

It is the structural engineer's challenge to decide to have the structure demolished or to have it rehabilitated. At this point, apart from technical issues, economical, cultural, social, and political factors may play a crucial role too. Due to high construction costs, need for much time and effort required for the

---

<sup>1</sup> Ast. Prof. Dr., Faculty of Civ. Eng., Istanbul Tech. Univ., Istanbul , Turkey, ailki@ins.itu.edu.tr

<sup>2</sup> Post. Grad. St., Faculty of Civ. Eng., Istanbul Tech. Univ., Istanbul, Turkey, esenyilmaz@softhome.net

<sup>3</sup> Research Assistant, Faculty of Civ. Eng., Istanbul Tech. Univ., Istanbul , Turkey, cdemir@ins.itu.edu.tr

<sup>4</sup> Prof. Dr., Faculty of Civ. Eng., Istanbul Tech. Univ., Istanbul , Turkey, kumbasar@ins.itu.edu.tr

reconstruction, seismic rehabilitation may appear to be more preferable in many cases. Seismic rehabilitation may have three aims: to recover original structural performance, to upgrade original structural performance, and to reduce seismic demand. In most cases upgrading the original structural performance may be necessary for existing structures built in 1960s and 1970s.

Deficiencies frequently observed in existing reinforced concrete moment-resisting frame systems are inadequate flexural strength and ductility of columns; inadequate shear strength of beams, columns, and beam-column joints; and poor anchorage and detailing of longitudinal and transverse bars. Many times these deficiencies are interrelated with each other. Non-ductile column confining zones of existing structures constructed with low strength concrete, inadequate transverse reinforcement and/or inadequate lap splice lengths are among the most commonly observed reasons for failures of structural members during earthquakes. Consequently, experimental and analytical research work on the behavior of these types of reinforced concrete structural members, and retrofit methods is vitally important for prevention and/or reduction of loss of lives and financial losses.

In order to cope with the widely observed failure of non-ductile potential plastic hinging regions many research works has been carried out. Since early 1990s efforts have been made to improve the behavior of plastic hinging regions by using external confining elements. Increase in the deformation capacity of plastic hinges through the passive confinement supplied by fiber reinforced polymer (FRP) wrapping has been a common topic of research, Saadatmanesh [2], Seible [3], Ye [4], Xiao [5].

Use of high performance cementitious materials for retrofitting of concrete members has also been studied. Researchers observed an improvement in terms of strength, ductility, energy dissipation characteristics, serviceability, and failure mode for concrete members retrofitted with high performance cementitious materials. Shannag [6] worked on the cyclic behavior of poorly detailed interior beam-column joints retrofitted with high performance steel fiber reinforced concrete jackets. Alaei [7] retrofitted damaged concrete flexural members by using CARDIFRC externally bonded high performance fiber reinforced cementitious composites. Shannag [8] used slurry infiltrated fibered concrete (SIFCON) jackets in order to increase shear capacity of reinforced concrete beams.

In this study, the behavior of non-ductile low strength concrete ( $f'_c=9.22$  MPa) column confining zones with or without adequate lap splices, and retrofit of these zones with prefabricated steel fiber reinforced concrete (SFRC) panel jackets are investigated. Experimental work, conducted at Istanbul Technical University (ITU) Structural and Earthquake Engineering Laboratory, consisted of 6 specimens tested under combined constant axial and reversed cyclic lateral loads. Nearly full scale 3 m high specimens with rectangular cross-sections represented the column parts between the mid-heights of succeeding stories. Similar original column units were also tested by other researchers, Paulay [9], Rodriguez [10], and Wu [11]. Longitudinal reinforcing bars of the 3 specimens were continuous, while the other 3 specimens had inadequate lap splices. One specimen with continuous and one specimen with lap spliced longitudinal reinforcement were tested as reference specimens. Potential plastic hinging zones of the other four specimens were retrofitted with prefabricated SFRC panels of two different thicknesses and panel connection details. Test results are presented in terms of strength, ductility, and failure mode characteristics. It was observed that the failure phenomena of the specimens with continuous and lap-spliced longitudinal reinforcement were quite different. Both reference specimens exhibited a poor performance especially in terms of ductility and failure mode. For retrofitted specimens significant behavioral improvement was obtained for strength, ductility, and failure mode.

## RESEARCH SIGNIFICANCE

This study is part of a research program to investigate the behavior of non-ductile column confining zones detailed with inadequate transverse reinforcement, low strength concrete, and plain reinforcing bars. Presence of inadequate lap splice length is also a parameter of the study. Easily applicable retrofit methods which can be used to improve the performance of existing reinforced concrete members were also examined. Considered type of structural elements are quite common not only in Turkey but also

worldwide, particularly in developing countries. Although there are many research works on retrofitting of existing rc elements, only a few of them consider non-ductile plastic hinging zones, low concrete strength and plain reinforcing bars. Moreover, the proposed retrofit method is quite feasible with its high constructability and high installation speed.

## THE PROBLEM

During severe earthquakes columns without sufficient transverse reinforcement detailed with adequate lap splice lengths for longitudinal reinforcement may encounter failure in a brittle manner, due to lack of confinement reinforcement. Concrete cover spalls and longitudinal bars buckle before the column reaches to the required displacement level that is imposed by the earthquake. In the case of poorly detailed lap spliced longitudinal bars, these bars may slide due to loss of bond causing an early decay in strength. Buckling or lap splice failures in the vicinity of beam-column joints may be followed by a rapid degradation in structure's lateral strength and stiffness, leading it to partial or even total collapse with a brittle mode of failure.

## SPECIMEN DESIGN

### Test Specimens

The selected prototype columns and joints were designed considering lower stories of a typical non-ductile moment-resisting frame of 1960s, 1970s. Generally, during design phase for the columns of lower stories of typical 4~5 story structures in Turkey, the level of dimensionless axial load is around 30%. However, since the actual concrete quality is worse than assumed during design phase, the dimensionless axial load level may increase significantly. Consequently for representing such cases the level of applied axial load varied between 37-47% of the axial force capacities of the specimens tested in the study. As in the case of actual existing structures, specimens were detailed with inadequate transverse reinforcements in order to form non-ductile potential plastic hinging regions. To represent majority of the existing structures built in 1960s and 1970s, specimens were cast using low strength concrete and plain bars for longitudinal reinforcement. Three of the specimens had continuous longitudinal reinforcing bars. The other three had lap-splices of 40×diameter of longitudinal bars, whereas the lap-splice lengths should have been around 145×diameter of longitudinal bars considering the actual yield strength of plain bars and concrete quality. According to the Turkish Standards TS500-2000 [12], lap splice length can be determined by using the design yield strength of the reinforcing bar ( $f_{yd}$ ) and the design tensile strength of the concrete ( $f_{ctd}$ ). Lap splice length,  $l_o$ , is directly related with the anchorage length,  $l_b$ , and can be calculated by Eq. (1)

$$l_o = c.l_b \quad (1)$$

where  $c=1.5$  if all lap splices are formed at the same section. The anchorage length for plain reinforcing bars can be calculated by Eq. (2)

$$l_b = 0.24.d.\frac{f_{yd}}{f_{ctd}} \quad (2)$$

where  $d$  is the diameter of the bar. According to these equations lap splice length should have been about 80×diameter (1120 mm) with the common design values of the materials of 1960s and 1970s (concrete characteristic compressive strength  $f'_c=14$  MPa, steel characteristic yield strength  $f_y=220$  MPa). However lap splice length was 40×diameter (560 mm) for these three specimens to examine the behavior of rc members with inadequate lap splice length. Note that as the actual yield strength of longitudinal bars was

higher and concrete compressive strength was lower than the values used for design, it should be considered that necessary lap splice length for the used materials was about  $145 \times \text{diameter}$ .

Other features of the original columns (concrete quality, arrangement of the longitudinal and transverse reinforcement) were same for all specimens. One specimen with continuous and one specimen with lap spliced longitudinal reinforcement were tested as reference specimens. Potential plastic hinging zones of the other four specimens were retrofitted with prefabricated SFRC panels of two different thicknesses and connection details.

The specimens represented the column parts between the mid-heights of successive stories. A central stub was formed to model beam column joints. Plastic hinging region formed at both sides of the central stub was specially detailed in order to be the testing zone. Specimens were nearly full scale with a cross-section of  $200 \times 300$  mm and height of 3 m. Plain reinforcing bars were preferred because they have been widely used in most of the existing structures in Turkey. Longitudinal bars had a diameter of 14 mm, while transverse bars had a diameter of 8 mm. Mechanical properties of reinforcing steel are given in Table 1. In this table,  $f_y$  and  $f_{su}$  are the yield and ultimate tensile strength of the reinforcement, while  $\epsilon_y$  and  $\epsilon_{su}$  are the yield and ultimate strains and  $f_s$  is the tensile strength of steel. The longitudinal reinforcement was hooked behind the supports and enclosed by transverse reinforcement. The spacing of transverse reinforcement was 200 mm in the testing zone and 100 mm out of the testing zone. Although 200 mm spacing for confinement was quite low compared with the quantities required by the recent building codes, it was enough to suppress a shear failure. In all column units geometric ratio of longitudinal reinforcement was  $\rho = 0.01$  and the volumetric transverse reinforcement ratio in the testing zone was  $\rho_h = 0.0037$ . Typical dimensions and reinforcing details of the reference column units are given in Fig. 1. For specimens R-C-SFRC-2 and R-LS-SFRC-2, support regions were wrapped with FRP layers. Clear cover was 20 mm for all column units.

**Table 1. Characteristics of the reinforcing bars**

Reinforcement	Diameter (mm)	$f_y$ (MPa)	$\epsilon_y$	$f_{su}$ (MPa)	$\epsilon_{su}$	$f_s$ (MPa)	Modulus of Elasticity (MPa)
Longitudinal	14	336	0.002	344	0.290	487	216000
Transverse	8	383	0.002	392	0.284	564	203000

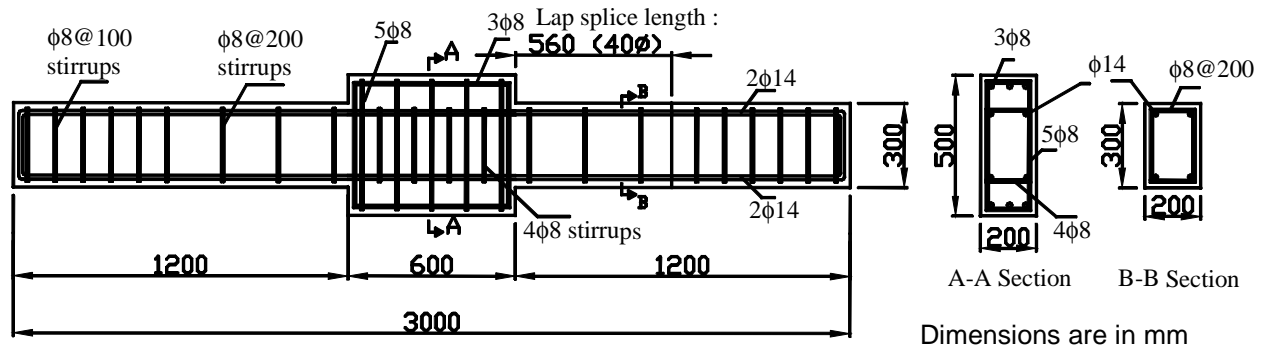


**Fig. 1. Details of the test specimens**

As the average concrete compressive strength for existing reinforced concrete structures in Turkey is approximately 10 MPa, Igarashi [13]. The target concrete compressive strength was 10 MPa. For construction of specimens, specially produced ready mixed concrete with water/cement ratio of 1.06 was used. Ordinary Portland cement (Set Marmara Cement) class 42.5 and fly ash from Catalagzi, Cayirhan were used in the mixture. Powdered stone and coarse aggregate were from Cebeci Dalbay with the maximum size of 0.7 and 15 mm, respectively. Sand was from Akpinar Sulun Mine with maximum size of

0.5 mm. Mid-range water reducer Grace WRDA 90W was used as superplasticizer in the mixture. Mix proportion is presented in Table 2. Compressive strengths were 9.22 MPa at 28 days, 12.96 MPa at 90 days, and 13.41 MPa at 150 days.

**Table 2. Concrete mix proportions (kg/m<sup>3</sup>)**

Cement	Water	Sand	Powdered Stone	Coarse Aggregate	Superplasticizer	Fly-ash
155	165	670	303	987	1.22	40

### Retrofit Procedure

Table 3 summarizes the properties of the tested specimens. In this table  $f'_{cj}$  is the cylinder compressive strength of the concrete at the specified ages. Note that  $0.85f'_{cj}$  ( $f'_{coj}$ ) corresponds to the concrete strength of the member. Axial force ratio ( $\nu$ ) was obtained by Eq. (3), where  $N$  is the applied axial force and  $A_g$  is the gross sectional area.

$$\nu = \frac{N}{0.85f'_{cj}A_g} \quad (3)$$

From a total number of 6 specimens, 4 were retrofitted with prefabricated steel fiber reinforced concrete (SFRC) jacket panels. More information on characteristics of that composite material is available elsewhere, Bayramov [14]. Mainly there were two retrofit groups in which the panel thicknesses and panel connection details were variables. First retrofit group was carried out with 30 mm thick SFRC jacket panels, and the second with 15 mm thick SFRC jacket panels. Specimen names give brief information about their basic features. For instance, R-C-SFRC-1 corresponds to a retrofitted (R) column that had continuous longitudinal reinforcement (C), and strengthened with SFRC jacket type 1. Similarly specimen R-LS-SFRC-1 had lap-spliced (LS) longitudinal reinforcing detail and retrofitted with SFRC jacket type 1.

**Table 3. Properties of the test specimens**

Specimen	Age (days)	$f'_{cj}$ (MPa)	$f'_{coj}$ (MPa)	$\nu$	Longitudinal Reinforcement Arrangement	SFRC Jacket Panel Thickness (mm)	SFRC Jacket Type (See Fig. 3)
C-O-1	51	10.6	9.0	0.47	Continuous	-	
LS-O-1	58	11.0	9.4	0.45	Lap spliced	-	
R-C-SFRC-1	185	13.4*	11.4	0.37	Continuous	30 mm	Type 1
R-LS-SFRC-1	199	13.4*	11.4	0.37	Lap spliced	30 mm	Type 1
R-C-SFRC-2	281	13.4*	11.4	0.37	Continuous	15 mm	Type 2
R-LS-SFRC-2	329	13.4*	11.4	0.37	Lap spliced	15 mm	Type 2

\*Concrete cylinder compressive strength at 150 days.

The total volumetric steel fiber ratio of the SFRC jacket panel mix was 4 percent. To optimize workability 10 mixture trials were done. The optimum SFRC mix-proportion obtained is presented in Table 4. As seen in this table, two types of steel fibers were used. Steel Fiber I (Dramix OL6/16) had a diameter of 0.16 mm and length of 6 mm, while the hooked end Steel Fiber II (Dramix ZP305) had 0.55 mm diameter and 30 mm length. Mechanical properties of the fibers are given in Table 5. The used microsilica was produced by Elkem Materials. Its mean particle size was smaller than 500  $\mu\text{m}$  with specific gravity of 2.3 kg/dm<sup>3</sup>. The admixture was Glenium 51 hyperplasticizer. Water/cement ratio was 0.25, and water/binder ratio was 0.22. Average compressive strength of SFRC at an age of 80 days was around 90 MPa, splitting tensile strength was around 10 MPa, and modulus of elasticity was around 37000 MPa. Mixing process was carried out in the following order: the coarsest particles (Silica Sand 1), the finest particles (microsilica),

next coarsest particles (Silica Sand 2), next finest particles (cement), short fibers and long fibers. After all dry ingredients were brought together, water and hyperplasticizer solution were added gradually to the dry mix. Mixing time was kept longer than an ordinary concrete. The SFRC jacket panels were cast in wooden forms and the forms were placed on vibration table to ensure satisfactory compaction. The panels were removed from their forms after one day and they were cured in water for six days.

**Table 4. SFRC mix-proportions (kg/m<sup>3</sup>)**

Cement	Water	Microsilica	Silica Sand-1	Silica Sand-2	Steel Fiber I (D=0,16, L=6)	Steel Fiber II (D=0,55, L=30)	Admixture
982.6	245.6	147.4	393	393	142.2	155.7	29.5

**Table 5. Mechanical properties of steel fibers**

Mechanical Properties of Dramix OL 6/16		Mechanical Properties of Dramix ZP 305	
Diameter, d (mm)	0.16	Diameter, d (mm)	0.55
Length, l (mm)	6	Length, l (mm)	30
Aspect Ratio (l/d)	37.5	Aspect Ratio (l/d)	55
Density (kg/dm <sup>3</sup> )	7.17	Density (kg/dm <sup>3</sup> )	7.85
Tensile Strength (MPa)	2250	Tensile Strength (MPa)	1100
Cover	Brass	Cover	N/A

An epoxy based adhesive, Degussa Concrevice 1406, was used to make SFRC panels adhere to column surfaces. This material has a tensile strength of 25 MPa and a compressive strength of 75 MPa at the age of 7 days. In order to improve the bond between retrofitting panels and column surfaces, surface preparation was carried out. Column surfaces were first roughened and a grid of diagonal grooves (3 mm depth at a spacing of 40 mm) was cut. Then all contact surfaces were cleaned carefully. After surface preparation the epoxy adhesive was applied on the prepared surface by a trowel to insure the uniform thickness of 4 mm of the epoxy layer. Panels of each column were installed in two successive days. Columns were in horizontal position while the panels were being installed to their side surfaces. Just after the installation process, panels were clamped to the columns. Retrofitted specimens are schematically shown in Fig. 2, SFRC panel jacket corner connection details are given in Fig. 3, and SFRC jacket panel installation steps are presented in Fig. 4.

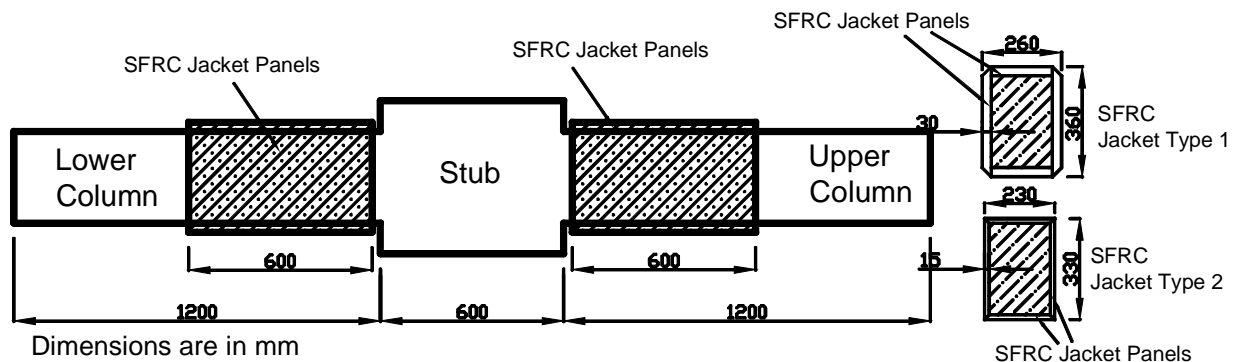


**Fig. 2. SFRC jacket types**

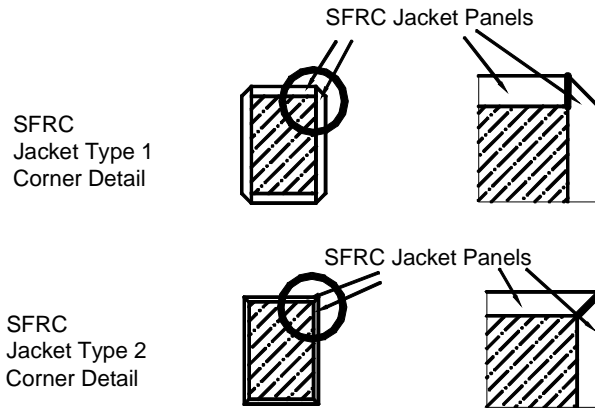


**Fig. 3. SFRC jacket corner connection details**

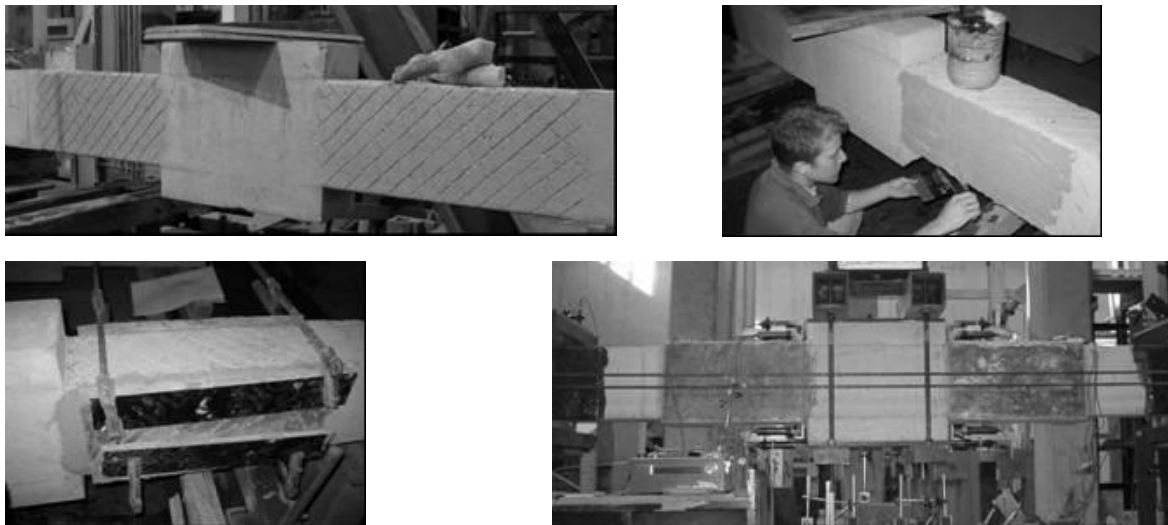


**Fig. 4. SFRC jacket panel installation**

## **TEST SETUP AND TESTING PROCEDURE**

### **Loading System**

The column units were tested at the Structural and Earthquake Engineering Laboratory of Istanbul Technical University. All specimens were tested under combined axial load and reversed cyclic lateral loads. Test setup is shown in Fig. 5, where it can be seen that the columns were tested in horizontal position. Steel rollers, profiles, plates, and rods were used to form the supports and the load transfer elements. Reversed cyclic flexural loads were applied vertically to the stub at the mid-heights of the specimens. A 250 kN capacity MTS servo-controlled hydraulic actuator was used to apply the lateral load and to perform the displacement controlled hysteresis loops.

A single curvature bending was obtained over the whole height of the specimens. This differs from the actual case in a moment-resisting frame, the input moments of the beams causes the sign of the curvature to be different above and below the beam-column joint. In tests investigating the beam-column joint cores, a method of loading that causes a change in the sign of the column curvature above and below the joint is necessary, because of the significant shear and bond stresses induced by the sign of the curvature. However, in tests investigating the behavior of the plastic hinge regions at the ends of the columns, the

simulation of the exact stress conditions in the beam-column joint core is not so important, Rodriguez [10], Park [15], Priestley [16].

Constant axial load was maintained by post-tensioning four ¾ inch (19.05 mm) diameter high strength cables with a hydraulic jack at one end of the specimens. A manually controlled 600kN Enerpac hydraulic jack was used for this purpose.

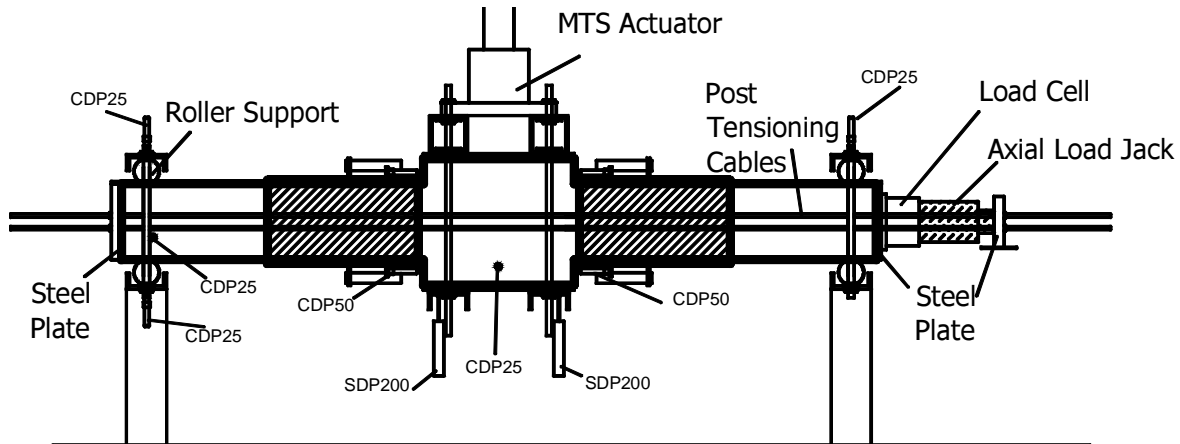


**Figure 5. Test setup**

### **Instrumentation**

Instrumentation system consists of linear variable displacement transducers (LVDT), internal and external load cells, and electrical resistance strain gages. Measurements from these instruments were acquired by a TML TDS-303 data logger via a TML ASW-50-C switch box. Lateral displacements and the rotation of central stub were measured with a pair of TML SDP-200D displacement transducers. All tests were conducted under displacement control, and control displacement was obtained by averaging these two transducers. At both sides of the stub, totally 12 TML CDP-50 displacement transducers with 50 mm stroke lengths were used to determine the average section curvatures. Bolts holding the curvature transducers were embedded into the core concrete, and stroke tips of these transducers were in contact with the stub faces. Curvatures of the potential hinging zones were measured over 150 and 300 mm gage lengths. Several other displacement transducers were also used to monitor reliability and safety of the experiments. Lateral flexural load acted by the MTS hydraulic actuator was measured with a 250 kN internal load cell, and the applied axial load was measured by a 1000kN TML CLP-100CMP load cell.

In order to measure the longitudinal and transverse reinforcement strains in the potential plastic hinging region, several strain gages were bonded on these bars. While most of them were TML YFLA-5 post-yield strain type measurement devices, a few were TML FLA-5 type ordinary foil gage. At peak displacement levels, the observed damage was recorded with photographs, videos, and sketches.

### **Loading Pattern**

At each test, a sequence of reversed cyclic flexural loads was applied combined with a constant axial load. Applied axial load was 252 kN for all specimens. This corresponds to a range of axial load ratios between 0.37 and 0.47 obtained by Eq. (3). This axial load ratio range is quite realistic especially for lower stories of structures with moment-resisting frames constructed with low strength concrete. After applying the axial load, the lateral displacements were imposed until the selected target levels. As shown in Fig. 6, the cyclic loading history can be divided into two phases. First phase, namely the elastic phase, included target displacements corresponding to drift ratios of  $\pm 0.0020$  ( $\pm 2.8$  mm),  $\pm 0.0025$  ( $\pm 3.5$  mm),  $\pm 0.0035$  ( $\pm 4.9$  mm), and  $\pm 0.0050$  ( $\pm 7.0$  mm). In the inelastic second phase, target displacements were determined according to the reference yield displacement,  $\delta_y$ . The  $\delta_y$  displacement was defined as the displacement of

the C-O-1 reference column at mid-height when the tension flexural reinforcement first yielded (9.5 mm). The columns were subjected to two pulling and pushing cycles at displacement ductility ratios of  $\mu = \pm 1.0, \pm 1.5, \pm 2.0, \pm 2.5, \pm 3.0, \pm 3.5, \pm 4, \pm 4.5, \pm 5, \pm 5.5, \text{ and } \pm 6$ , where  $\mu$  is the displacement ductility factor defined as  $\delta/\delta_y$ .  $\delta$  was the average lateral displacement of the central stub. Ductility displacement ratio,  $\mu = \pm 6.0$  could only be applied in the case of continuously reinforced specimens.

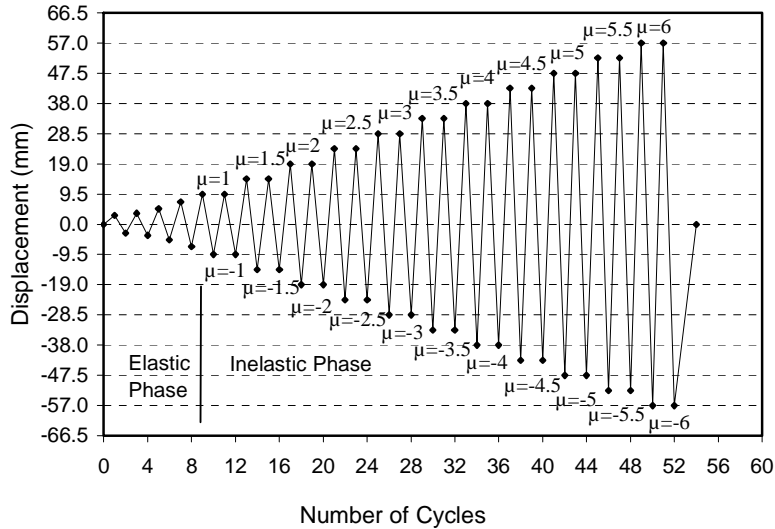


**Fig. 6. Loading pattern**

### TEST RESULTS

#### Specimen C-O-1

This is the reference specimen with continuous longitudinal bars. The lateral load versus lateral displacement hysteresis loops measured at the stub is shown in Fig. 7. All load-displacement relationships were obtained considering the load acted by the MTS hydraulic actuator and the average displacement measured under the stub.

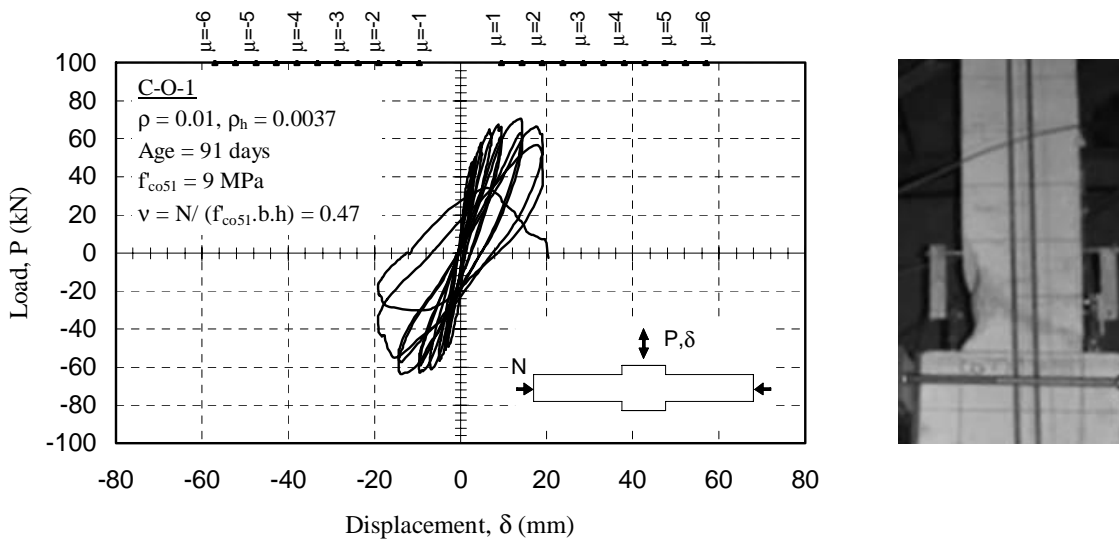


**Fig. 7. Load-displacement relationship and damage pattern for C-O-1**

First flexural cracks were observed at a displacement of 2.8 mm (0.002 drift ratio). In the following elastic cycles, cracks were scattered on both upper and lower columns through the first 300 mm zones from the stub faces. After the displacement ductility level of  $\mu = 1.0$  (9.5 mm) cracks were concentrated and widened in the first 150 mm zone of both columns. At the displacement ductility level of  $\mu = \pm 1.5$  ( $\pm 14.25$  mm) concrete crushing was observed at a load level of 71 kN. In the following cycles cracks concentrated on the lower column and at the first cycle of displacement ductility level  $\mu = -2.0$  (-19 mm), lower column concrete cover spalled. At the second cycle of displacement ductility level  $\mu = -2.0$  (-19 mm), significant strength degradation was observed due to buckling of the longitudinal bars in the lower column. While loading was going on for the next target displacement ductility level of  $\mu = 2.5$  (+23.75 mm), longitudinal bars of the upper column buckled at the displacement level of +14 mm and test was stopped due to very high level of strength degradation. Damage pattern for specimen C-O-1 is given in Fig. 7.

### Specimen LS-O-1

This is the reference specimen with lap spliced longitudinal bars in the upper column. The lateral load versus lateral displacement relationship is given in Fig. 8. After the displacement level of +7 mm, cracks were concentrated on the upper column where lap splice was located. At displacement level +9.5 mm, 54 kN maximum load was observed. At the second cycle of displacement ductility level  $\mu = \pm 1.0$  ( $\pm 9.5$  mm), longitudinal cracks at the end of the lap splices were observed due to reinforcement slip. At the displacement ductility level of  $\mu = \pm 1.5$  ( $\pm 14.25$ ) concrete crushing was observed. During the cycles of ductility levels of  $\mu = \pm 2.0$  ( $\pm 19$  mm) concrete cover spalled. Test was stopped at the second cycle of displacement ductility level of  $\mu = -2.0$  (-19 mm). Damage pattern is given in Fig. 8.

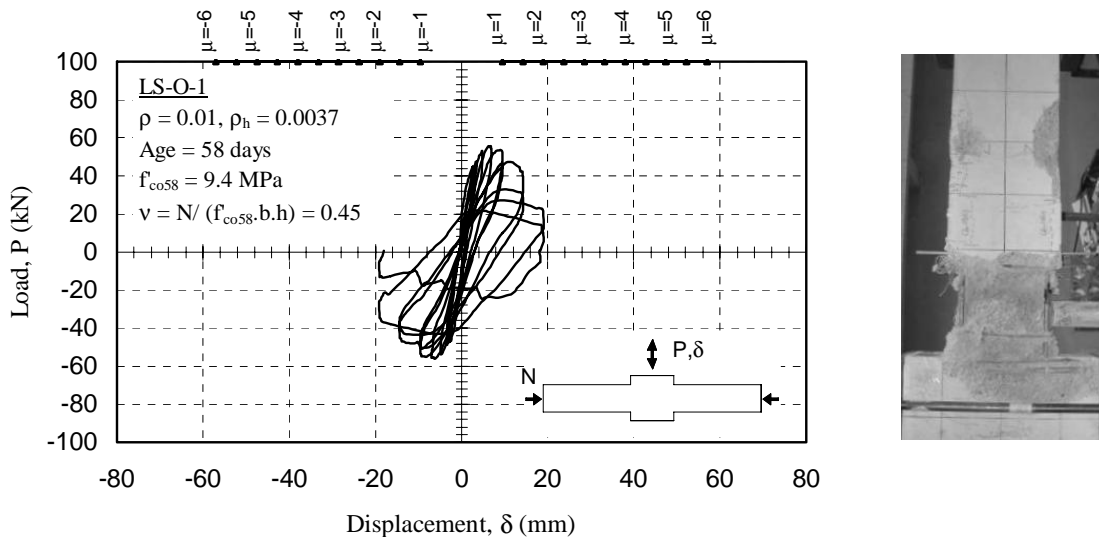


**Fig. 8. Load-displacement relationship and damage pattern for LS-O-1**

### Specimen R-C-SFRC-1

Specimen R-C-SFRC-1 with continuous longitudinal reinforcement was retrofitted with prefabricated SFRC jacket panels of 30 mm thickness. The lateral load versus lateral displacement relationship measured at the stub is shown in Fig. 9. First bending crack was observed in the critical section at  $\delta = 1.55$  mm ( $F = 48$  kN) in pushing and at  $\delta = -1.1$  mm ( $F = -47$  kN) in pulling. After the drift ratio of 0.005, damage was concentrated at the lower column. At the displacement ductility ratio of  $\mu = 3.5$  (33.25 mm), damage was observed at the support. Cracks at the connections of the retrofitting panels were observed after the ductility ratio of  $\mu = 3.5$  (33.25 mm). At further displacement levels, the cracks at the connections

of the retrofitting panels tended to widen and extend. As the cracks got wider and extend, decrease in the capacity of the specimen was observed. Buckling of the longitudinal reinforcement was prevented by the effect of confinement provided by the SFRC jacket. The increase in the load capacity of specimen R-C-SFRC-1 with respect to the reference specimen C-O-1 was 20 percent in pushing and 47 percent in pulling. At the end of the test, the decrease in the strength of the specimen was 25 percent in pushing and 38 percent in pulling. R-C-SFRC-1 specimen at the end of the test is shown in Fig. 9.

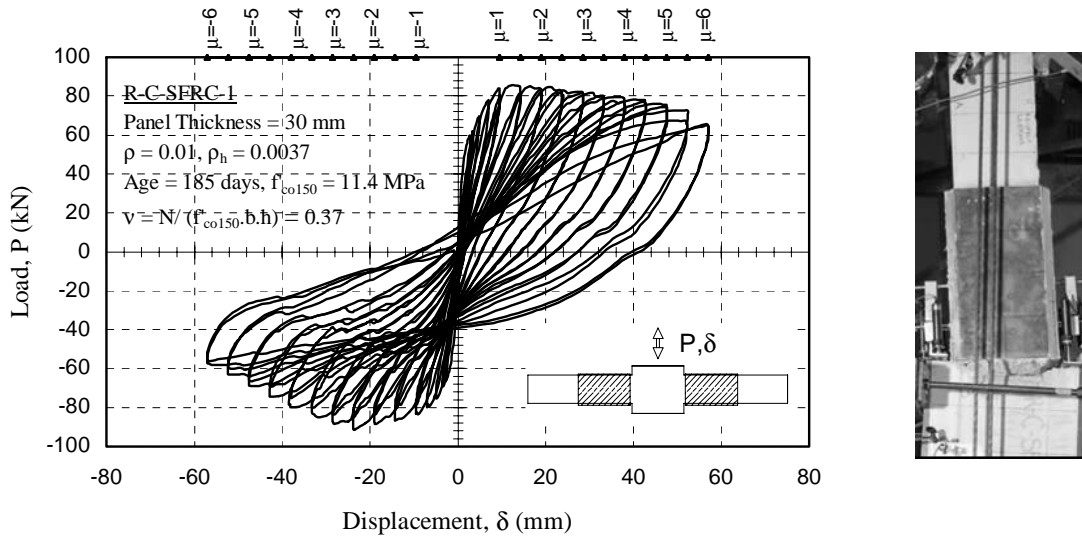


**Fig. 9. Load-displacement relationship and damage pattern for R-C-SFRC-1**

### Specimen R-C-SFRC-2

Specimen R-C-SFRC-2 with continuous longitudinal reinforcement was retrofitted with prefabricated SFRC jacket panels of 15 mm thickness. The lateral load versus lateral displacement hysteresis loops measured at the stub is shown in Fig. 10.

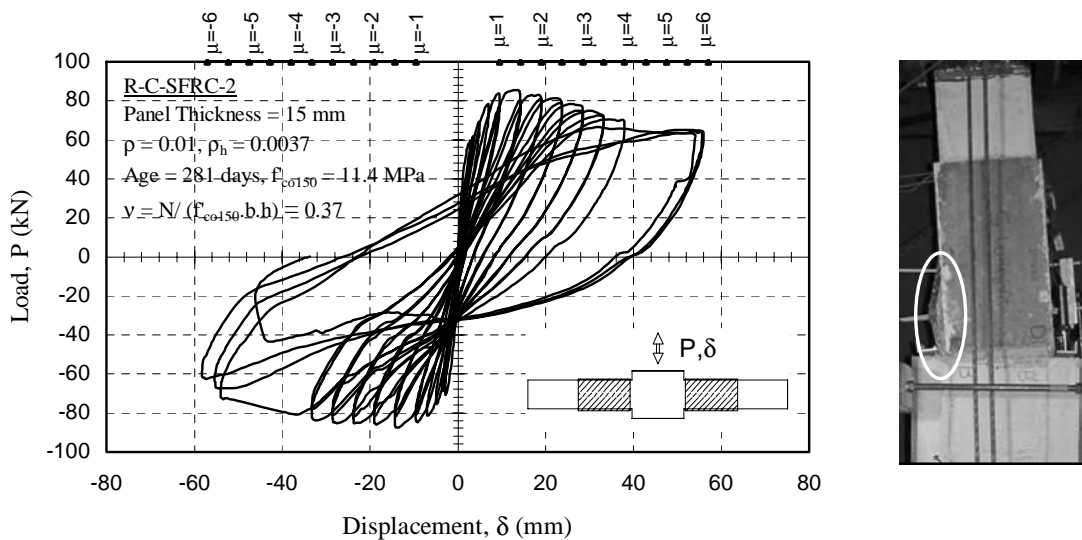


**Fig. 10. Load-displacement relationship and damage pattern for R-C-SFRC-2**

First bending crack was observed in the critical section at  $\delta=1.7$  mm ( $F=49$  kN) in pushing and at  $\delta=-1.6$  mm ( $F=-56$  kN) in pulling. The damage was concentrated mainly in the plastic hinge region above the

central stub in pushing and in the plastic hinge region below the central stub in pulling after the displacement ductility ratio of  $\mu=2.5$  (23.75 mm). First crack at the panel connection near the stub formed in the displacement ductility level of  $\mu=1.5$  (14.25 mm). The actuator went out of control while approaching the displacement level of -38 mm. Consequently for that cycle, the peak displacement was -54 mm instead of -38 mm. At this displacement level, at the support of the upper column a crack was observed through the longitudinal reinforcement. In the last cycle of displacement ductility ratio of  $\mu=6.0/2$  (-57 mm), longitudinal reinforcement and the retrofitting panel of the lower column buckled, Fig.10. The increase in the load capacity of specimen R-C-SFRC-2 with respect to the reference specimen C-O-1 was 20 percent in pushing and 40 percent in pulling. At the end of the test the decrease in the strength of the specimen was 27 percent in pushing and 50 percent in pulling.

### Specimen R-LS-SFRC-1

Specimen R-LS-SFRC-1 with lap spliced longitudinal reinforcement was retrofitted with prefabricated SFRC jacket panels of 30 mm thickness. The lateral load versus lateral displacement hysteresis loops measured at the stub is shown in Fig. 11. First bending crack was observed in the critical section at  $\delta=1.3$  mm ( $F=45$  kN) in pushing and  $\delta=-2$  mm ( $F=-61$  kN) in pulling. The damage was concentrated mainly in the plastic hinge region above the central stub, where lap splice was located, after the displacement ductility ratio of  $\mu = 1.0$  (9.5 mm).

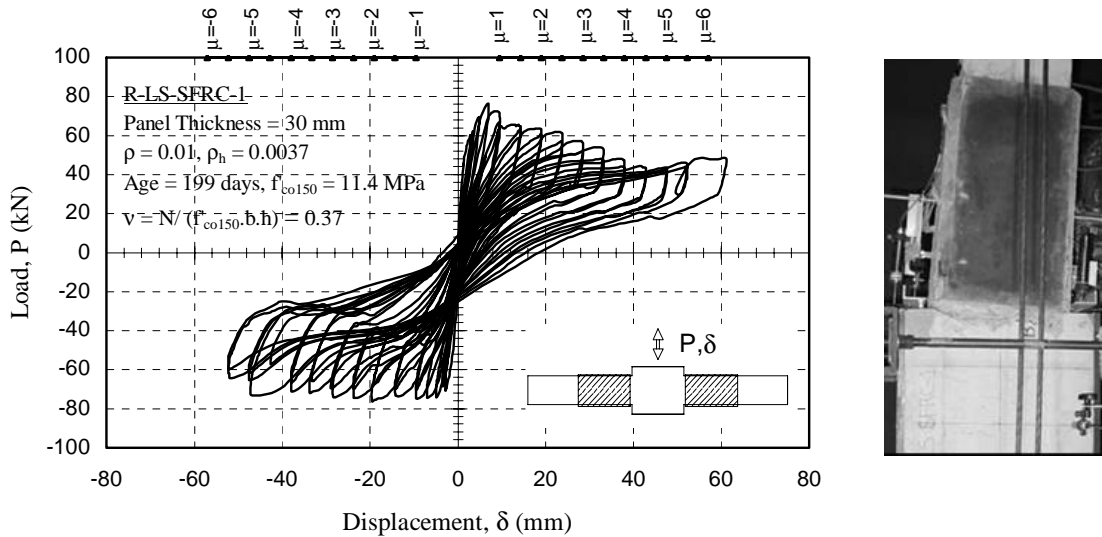


**Fig. 11. Load-displacement relationship and damage pattern for R-LS-SFRC-1**

Cracks at the panel connection above the stub were formed in the displacement ductility level of  $\mu = 2.5$  (23.75 mm). However the strength started to degrade before the cracks were formed at the connections of the panels. Strength degradation in pushing was steeper than pulling. The increase in the load capacity of specimen R-LS-SFRC-1 with respect to the reference specimen LS-O-1 was 41 percent in pushing and 36 percent in pulling. At the end of the test the decrease in the strength of the specimen was 43 percent in pushing and 21 percent in pulling. Damage pattern is given in Fig. 11.

### Specimen R-LS-SFRC-2

Specimen R-LS-SFRC-2 with lap spliced longitudinal reinforcement was retrofitted with prefabricated SFRC jacket panels of 15 mm thickness. The lateral load versus lateral displacement hysteresis loops measured at the stub is shown in Fig. 12. First bending crack was observed in the critical section at  $\delta=1.3$  mm ( $F=43$  kN) in pushing and  $\delta=-1.45$  mm ( $F=-45$  kN) in pulling. The damage was concentrated mainly

in the plastic hinge region above the central stub, where lap splice was located, after the displacement ductility ratio of  $\mu=1.0$  (9.5 mm). Cracks at the panel connection above the stub formed at the displacement ductility level of  $\mu=1.5$  (14.25 mm). A significant difference was observed between load capacity in pulling and pushing. Steep strength degradation in both pulling and pushing cycles was observed. At the displacement ductility ratio of  $\mu=-5.0/1$  a crack formed both at the end of the lap splice and SFRC jacket panel connections. At the displacement ductility ratios of  $\mu=\pm 5.5$  longitudinal reinforcement of the upper column buckled. The increase in the load capacity of specimen R-LS-SFRC-2 with respect to the reference specimen LS-O-1 was 17 percent in pushing and 52 percent in pulling. At the end of the test the decrease in the strength of the specimen was 83 percent in pushing and 63 percent in pulling. Damage pattern is given in Fig. 12.

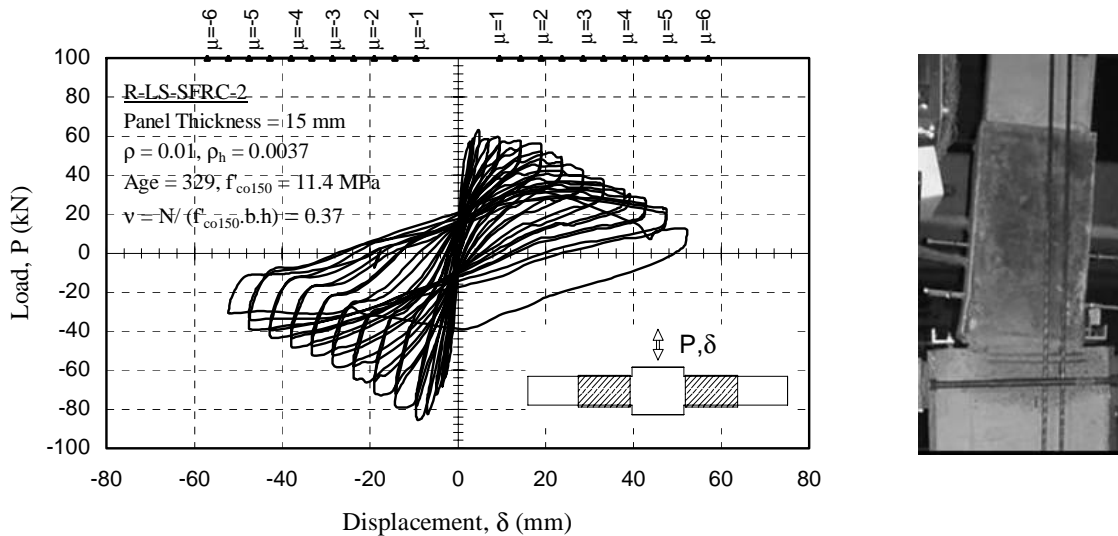


**Fig. 12. Load-displacement relationship and damage pattern for R-LS-SFRC-2**

## DISCUSSIONS

Reference specimen with continuous longitudinal reinforcement exhibited premature failure due to buckling of the longitudinal bars while loss of bond caused premature failure for the reference specimen with inadequate lap splice length.

Both specimens R-C-SFRC-1 and R-C-SFRC-2 behaved similarly and exhibited an improved behavior in terms of ductility, strength, and failure mode. This showed that for specimens with adequate lap splices 15 mm thick SFRC jacket panels provided similar enhancement as 30 mm thick SFRC jacket panels, see Fig. 13. At the displacement ductility level of  $\mu=+2$ , the percentage of strength degradation was 13% for specimen C-O-1, 2% for specimen R-C-SFRC-2, whereas there was no strength degradation for R-C-SFRC-1. Note that the specimen C-O-1 failed just after the ductility level of  $\mu=2$  due to buckling of the longitudinal bars. At the end of the tests ( $\mu=+6$ ) percentage of strength degradation was 25% for specimen R-C-SFRC-1, and 27% for R-C-SFRC-2.

Lap spliced specimens had steeper strength degradations because loss of bond occurred even with very small amount of transverse strains of concrete. In the case of retrofitted lap spliced specimens; R-LS-SFRC-1 with the jacket thickness of 30 mm performed better than R-LS-SFRC-2 with the jacket thickness of 15 mm, see Fig. 13. Although an increase in the strength was observed for the specimen retrofitted with SFRC jacket panels with thickness of 15 mm, that strength could not be sustained along the test. At the displacement ductility of  $\mu=+2$ , percentage of strength degradation was 63 percent for specimen LS-O-1, 17 percent for specimen R-LS-SFRC-1, and 11 percent for R-LS-SFRC-2. Specimen LS-O-1 failed just

after the ductility level of  $\mu=2.5$  due to excessive loss of bond. At the end of tests ( $\mu=+5.5$ ) percentage of strength degradation was 43 percent for specimen R-LS-SFRC-1, and 83 percent for R-LS-SFRC-2. Note that due to bond slip, there is a significant pinching in the load-displacement relationships of retrofitted specimens with inadequate lap splices, particularly R-LS-SFRC-1.

The increase in the strength and the failure modes of the specimens are summarized in Table 6. Specimens retrofitted with SFRC jacket panels with thickness of 30 mm prevented buckling of the longitudinal reinforcement and significantly delayed loss of bonding.

It was observed that the flexural rigidities of the rc members was not significantly affected with the installation of SFRC jacket panels. Consequently, only minor changes may be expected in the dynamic characteristics of the structure retrofitted with this technique.

**Table 6. Summary of test results**

Specimens	Maximum Load (kN)		Increase in Strength		Failure Mode
	Pushing	Pulling	Pushing	Pulling	
C-O-1	71	-62	-	-	Buckling of longitudinal reinforcement
LS-O-1	54	-56	-	-	Loss of bond
R-C-SFRC-1	85	-91	0.20	0.47	Slight degradation in strength
R-LS-SFRC-1	76	-76	0.41	0.36	Loss of bond
R-C-SFRC-2	85	-87	0.20	0.40	Slight degradation in strength, buckling of longitudinal reinforcement
R-LS-SFRC-2	63	-85	0.17	0.52	Loss of bond

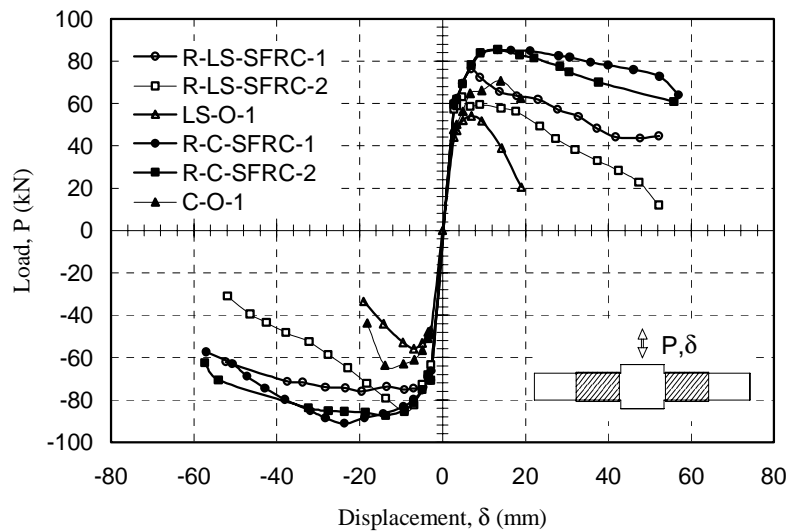


**Fig. 13. Experimental load-displacement envelopes for continuous and lap spliced specimens**

## CONCLUSIONS

The purpose of this study was to investigate the behavior of non-ductile low strength rc columns with or without adequate longitudinal reinforcement lap splice length and to examine a new retrofitting technique. The proposed retrofitting was carried out by externally bonding prefabricated SFRC jacket panels to the column faces at potential plastic hinging zones. High production and installing speed supplied by prefabrication is a significant advantage of this technique. No matter the longitudinal reinforcement is continuous or lap spliced, investigated retrofit technique improved the behavior significantly in terms of ductility and strength. The enhancement in the behavior was more pronounced in the case of the specimens without inadequate lap splices. Note that attention should be paid to the bonding of the SFRC

jacket panels to the column surfaces and to each other at the jacket corners. As the flexural rigidities of the rc members were not increased with the installation of the SFRC jacket panels, possible detrimental effects to the dynamic characteristics of the structure retrofitted by this method are minimized.

### ACKNOWLEDGMENTS

The research described in this paper was funded by The Scientific and Technical Research Council of Turkey (TUBITAK) and Yapkim-Degussa Construction Chemicals Company. Valuable contributions of Prof. Dr. M.A. Tasdemir, Beksa Company, Izola Construction Company, Mr. V. Koc and Ms. A. Tezcan are also gratefully appreciated.

### REFERENCES

1. US Geological Survey (USGS) web site, "www.usgs.gov".
2. Saadatmanesh H, Ehsani MR, Jin L. "Repair of earthquake-damaged rc columns with FRP wraps." *ACI Structural Journal* 1997; 94(2): 206-215.
3. Seible F, Priestley MJN, Hegemier GA, Innamorato D. "Seismic retrofit of rc columns with continuous carbon fiber jackets." *Journal of Composites for Construction* 1997; 1(2): 52-62.
4. Ye LP, Zhang K, Zhao SH, Feng P. "Experimental study on seismic strengthening of rc columns with wrapped CFRP sheets." *Construction and Building Materials* 2003; 17: 499-506.
5. Xiao Y, Ma R. "Seismic retrofit of rc circular columns using prefabricated composite jacketing." *Journal of Structural Engineering* 1997; 123(10): 1357-1364.
6. Shannag MJ, Barakat S, Abdul-Kareem M. "Cyclic behavior of HPFRC-repaired reinforced concrete interior beam-column joints." *Materials and Structures* 2002; 35: 348-356.
7. Alae FJ, Karihaloo BL. "Retrofitting of reinforced concrete beams with CARDIFRC." *Journal of Composites for Construction* 2003; 7(3): 174-186.
8. Shannag MJ, Barakat S, Jaber F. "Structural repair of shear-deficient reinforced concrete beams using SIFCON." *Magazine of Concrete Research* 2001; 53(6): 391-403.
9. Paulay T. "Lapped splices in earthquake-resisting columns." *ACI Journal* 1982; 79: 458-469.
10. Rodriguez M, Park R. "Seismic load tests on reinforced concrete columns strengthened by jacketing." *ACI Structural Journal* 1994; 91(2): 150-159.
11. Wu YF, Griffith MC, Oehlers DJ. "Improving the strength and ductility of rectangular reinforced concrete columns through composites partial interaction: Tests." *Journal of Structural Engineering* 2003; 129(9): 1183-1190.
12. "Requirements for design and construction of rc structures (TS500-2000)." Turkish Standards Institute, Ankara, 2000.
13. Igarashi S. "Recommendations on minimizing earthquake damage in big cities in Turkey". *Proceedings of ITU-IAHS International Conference on the Kocaeli Earthquake, Istanbul, Turkey.* Istanbul: Istanbul Technical University, 1999.
14. Bayramov F, Aydoner T, Ilki A, Tasdemir C, Tasdemir MA. "An optimum design for steel fiber reinforced concretes under cyclic loading". *Fifth International Conference on Fracture Mechanics of Concrete and Concrete Structures & Post-Conference Workshop, Vail Colorado, USA, 2004, (accepted for publication).*
15. Park R. "Evaluation of ductility of structures and structural assemblages from laboratory testing." *Bulletin of the New Zealand National Society for Earthquake Engineering* 1989; 22(3): 155-166.
16. Priestley MJN, Park R. "Strength and ductility of concrete bridge columns under seismic loading." *ACI Structural Journal* 1987; 84(1): 61-76.